Evaluation of a New Dispersion Technique for Assessing Triboelectric Charging of Powders

U. Zafar, F. Alfano[1], and M. Ghadiri[*]

School of Chemical and Process Engineering, University of Leeds, Leeds LS2 9JT, UK

*Corresponding author: M.Ghadiri@leeds.ac.uk

Abstract

In a number of applications, especially in pharmaceutical drug development, there is often a very small powder quantity available for evaluating the manufacturability of new drugs. However, it is highly desirable to be able to quickly evaluate processing issues, and where possible using the smallest powder quantity. In the present work, a proprietary commercial powder dispersion device (the disperser of Malvern© Morphologi G3) is adapted to evaluate the triboelectric charging tendency. A very small powder quantity (as small as 0.1 mg) is dispersed by a pressure pulse of compressed gas such as air or nitrogen. This causes the particles to become air borne and collide with the containing walls, resulting in dispersion and leading to triboelectric charge transfer between the particles and the walls. In this work, the charging propensity of a number of materials is evaluated and the effect of particle surface functional groups on the tribo-electric charge transfer is analysed. Model materials with a well-defined shape (glass ballotini) but with different silane groups deposited on their surfaces as well as a number of organic crystalline particles (such as aspirin, α-lactose monohydrate and paracetamol) are tested. Following dispersion the particles move immediately to a Faraday cup placed directly underneath the disperser. Therefore, particle charge is measured with no decay. The method can differentiate charging of different polymorphs of the same material, different silane groups on the surfaces of glass ballotini and different crystal morphologies obtained from crystallisation from various solvents.

---

[1] On Erasmus Exchange Programme from Universita della Calabria, Arcavacata di Rende (CS), 87030, Italy.

1. Introduction

Powders often become triboelectrically charged by particle-particle and particle-surface collisions in various industrial operations, such as pneumatic conveying, comminution and mixing. In the pharmaceutical industry, organic crystals are very prone to triboelectric charging. They usually have a high bulk electrical resistance and therefore, electrostatic charges can accumulate and have adverse effect on flowability, adhesion and segregation, leading to content non-uniformity in formulation, batch failures and manufacturing delays (Pingali et al., 2009), (Hoe et al., 2009), (Wong et al., 2014) and (Naik et al., 2016).

There are three main mechanisms by which tribo-electric charging can take place, i.e. electron, ion and material transfer (Matsusaka et al., 2010). Charge transfer is the result of differences in the work function of two materials in contact (Harper, 1967; Elsdon and Mitchell 1976; Itakura et al., 1996; and Matsusaka et al., 2010). However, for materials other than electrical conductors, the prediction of charge transfer from a theoretical base is difficult, and hence the approach is largely empirical (Gupta et al., 1992; and Matsusaka et al., 2010). The work function of a powder depends on its physical and chemical properties including environmental conditions (Yurteri et al., 2002; Matsusaka and Masuda. 2003; Watano, 2006; Kwek et al., 2012; He et al., 2014; Karner et al., 2014; and Mukherjee et al., 2016).

A number of methods have been developed to characterise the charging propensity of powders, based on different mechanistic principles (Matsusaka et al., 2010). The Faraday cage method is widely used for measuring the electrostatic charge on powders (Chilworth Instruments, Southampton, UK). It has been used in different ways to measure the resultant charge for bulk

powders in a number of studies, i.e. Brown, (1997), Rowley (2001), Chow et al. (2008), Sarkar et al. (2012), Šupuk et al. (2012), Zarrebini et al. (2013), Karner et al. (2014). However, these setups can only be used for net charge measurement and cannot quantify charge distribution in multicomponent systems. Several studies have reported charge transfer due to the collision of a single particle against a target, e.g. Masuda and Iinoya (1978), Masui and Murata (1983), Matsuyama and Yamamoto (1995), Matsusaka et al. (2000), Zhao et al. (2002), Ema et al. (2003), Watanabe et al. (2007). Hussain et al. (2016) used a series of Faraday cages mounted vertically in cascade to monitor triboelectrification in a fluidised bed and pneumatic transport system. This approach allowed the study of charge distribution in a bipolar system as a function of different process parameters. Recently, Smyth et al. (2004), Kwek et al. (2012), Zhou et al. (2013) and Biegaj et al. (2016) employed a non-intrusive procedure involving an oscillating vibrating capacitive probe based on the method of Masuda et al. (1995), to measure the contact potential difference and to investigate triboelectric chargeability of pharmaceutical powders under controlled environmental conditions.

Kwok et al. (2005), Telko et al. (2007) and Ali et al. (2008) used an Electrical Low Pressure Impactor (ELPI) to measure the triboelectric charging for aerosols. The cascade setup of ELPI detects particle deposition by measuring the electrical current resulting from the dissipation of particle charge via a multichannel electrometer. However, the technique is dependent on particle density as well as size which affects the impact location of each particle, compromising the measurement precision for size-number distribution (Coudray et al., 2009). Furthermore, it is limited to fixed station sampling due to its size and weight. Murtomaa et al. (2003) and Saini et al. (2008) used the ESPART device to measure charge to mass ratio of individual particles of aerosol. The device generates an oscillating electric field that causes particles to oscillate and provide information on the particle charge-to-mass ratio. The technique has been used to

study bipolar charging for micrometre size range particles, and interactions between inhaler surfaces and formulation. However, issues with particle detection and analysis system through the sensing volume may occur due to the electric field caused by inhomogeneous geometry (Epping and Kuettner 2002). Another novel instrument used by Yli-Ojanpera et al. (2014), Wong et al. (2015) and Leung et al. (2016) is Bipolar Charge Analyser (BOLAR^{TM}). It consist of a flow divider that distributes the flow evenly to five bipolar detectors based on the particle size range for charge measurement. Each detector has two cylinders with the inner cylinder maintained at high positive potential whilst the outer cylinder is grounded to create an electric field between them. The electric current signals from each cylinders are integrated over the measurement period to calculate the charge value. However, the accuracy of the measurements depends on the effectiveness of flow division upon entering the detector cylinders. A summary of the techniques has been given by Matsusaka et al. (2010) and Naik et al. (2016).

In this work, the focus is on characterising the triboelectric charging tendency of fine powders by impact using the smallest possible sample quantity. The dispersion unit of Malvern ® Morphologi G3 is used for this purpose. The method is based on the aerodynamic dispersion by a pressure pulse, making the particles airborne and impacting them on the containing walls. This causes charge transfer as the walls are made of materials with different work functions, thereby enabling the charging propensity of the powder and its position in the triboelectric series to be evaluated. The dispersed powder is immediately discharged into a Faraday cage, preventing any charge decay. Recently Ali and Ghadiri (2017) analysed the charging mechanism of this method using Computational Fluid Dynamics (CFD) and Lagranian particle tracking, showing the potential of the method for assessing the charging propensity of powders. The salient conclusions of their work are that particles impact a number of times, around 10 times on average, within the disperser before getting out and the level of charge is insensitive

to the pressure pulse magnitude, implying that the equilibrium charge level is roughly attained. Here we evaluate this method for assessing the charging tendency of various powders, such as active pharmaceutical ingredients and excipients as well as surface-treated glass ballotini to explore whether this method can characterise and differentiate the powders with deliberate and well-controlled changes, e.g. different polymorphs, morphologies and surface functional groups.

2. Method and Materials

The dispersion setup is shown in Figure 1. There are three main components: dispersion cap, post-dispersion duct and dispersion capsule. The dispersion cap is made of stainless steel. It houses the dispersion capsule and connects the unit to a compressed air line. The post-dispersion duct is used to mount the dispersion capsule onto it and is made of the same material as the capsule. Rubber rings are used to seal the gap between the capsule and duct during the dispersion process. The capsule and post-dispersion duct are made of materials of choice to establish the relative position of the test powder according to the triboelectric series. In this work they were made of stainless steel, copper, brass, aluminium and PTFE (as shown in Figure 2). The bottom section of the post-dispersion duct consists of a cylindrical section, which acts as a passage way for the particles to exit the disperser. It is used to mount the dispersion unit on to Faraday cage for charge measurement. It should be noted that in the normal setup of the G3 disperser all the components are made of stainless steel. It is only in this work and for the first time that materials with different work function are tried to establish to position of the powders of interest in the table of triboelectric series. The dispersion capsule consists of two sections sealed by an O-ring as shown in Figure 3. The sample powder is housed in the central sample well. When an air pressure pulse is applied, particles are pushed radially outwards in

the well and lifted due to the presence of a small lip around the sample well. They then impact on the top section and bounce back and may again hit the bottom section. The impact and bouncing process continue until the particles leave the capsule from the small rounded holes, getting charged as a result of collisions. They then immediately enter the Faraday cage connected to an electrometer, by which the net charge is measured. The sample is added to the capsule in a volumetric amount using sampling spoons designed for this purpose and supplied by Malvern® Instruments Ltd.

Laboratory compressed air was used for dispersion. Pipes used for connections were anti-static in order to remove the possibility of the pipe becoming electrostatically charged during repeated testing. The operation pressure and injection time of the pressure pulse were controlled using a pressure regulator (SMC, Model 2030-212BLA) and a solenoid valve (SMC, Model VQ21A1). The airflow was filtered (SMC, Model AF20-F02C) to remove particulate impurities like oil droplets and dust particles. The Faraday inner cup was connected to an electrometer (Keithley, Model 6541, USA) which had a resolution of 10 pC, via a low noise BNC cable, whilst the outer cup was earthed. The charge measurement setup is shown in Figure 4.

Organic and inorganic particles were used for exploring the potential of the method for assessing the tribocharging propensity. These included aspirin, α-lactose monohydrate, paracetamol, urea, L-glutamic acid, carbamazepine and glass ballotini, model material of well-defined shape. The glass ballotini were acid washed and sieved into three narrow particle size cuts of 53-63 µm, 75-80 µm and 106-112 µm. This narrow range was achieved by combining the British and German standard sieves together in order to reduce the width of size distribution, thereby reducing its effect on the charge measurement. The size distributions of the selected

test materials were measured by laser diffraction using the wet dispersion mode of the Malvern Mastersizer 2000. The results are shown in Table 1 for glass ballotini and in Table 2 for aspirin and α-lactose monohydrate. All the experiments reported in this study were carried out at 23±3 °C and relative humidity range of 37±4 %. For each given material and condition, at least five repeats were carried out. The maximum and minimum values of charge-to-mass ratio is represented by an error bar on the data points.

3. Results and Discussion

Effect of Particle Size

The effect of particle size on triboelectric charging is investigated using the three sieve size cuts of glass ballotini, as a function dispersion pressure. A constant sample volume of about 3 mm^3 is used. Multiple measurements of particle size distribution by laser diffraction are made (10 for each sample) and the characteristic measures of particle sizes distribution, i.e. in terms of D_{10}, D_{50} and D_{90} along with the Sauter diameter D[3,2] (the diameter of a sphere with the volume to surface area ratio that is equivalent to that of the particles of interest) are given in Table 1.

The results of triboelectric charging are expressed in absolute value of charge-to-mass ratio as a function of dispersion pressure against stainless steel contacting surfaces, and the average measurement of at least five repeats for each case is shown in Figure 5. All the sieve cuts of glass ballotini tested in the above measurement charged negatively after contacting with stainless steel which is in agreement with Zarrebini et al. (2013). The result in Figure 5 shows that the charge-to-mass ratio is larger for smaller glass ballotini sizes. This is due to the increase in the total surface area of the sample in a given volume (Harper 1967), (Sarkar et al., 2012)

and (Mukherjee et al., 2016). Furthermore, it is noteworthy the charge-to-mass ratio remains independent for the dispersion pressure range tested (0.5-3 barg). The specific surface area of the size cuts from laser diffraction analysis (LDA), and the charge per unit surface area are given in Table 1. It is noteworthy that the charge per unit surface area decreases almost linearly with particle size D[3,2].

Effect of Sample Volume

The effect of sample volume on triboelectric charging was evaluated by testing glass ballotini of sieve cut 53-63 µm against the stainless steel surface using bulk volumes of 1, 3, 5, 7 and 9 mm^3 at 2 barg dispersion pressure. The results obtained for absolute value of charge-to-mass ratio as a function of sample volume are shown in Figure 6.

A decrease in the charge-to-mass ratio is observed for sample volumes of 7 and 9 mm^3, whilst it remains constant for the smaller volumes (i.e. 1, 3 and 5 mm^3). This trend is likely due to the 'space charge effect' (Matsusaka et al. 2010), enhanced by the increase in the particle number for larger sample volumes. This promotes inter-particle collisions, which as compared to particles-wall collisions, brings about reduced charge transfer.

Effect of wall material surface

The charge polarity and magnitude acquired by the particles depend on the work function of the contacting surfaces. In order to evaluate the effect of surface material on triboelectric charging due to dispersion, five different materials (stainless steel, copper, brass, aluminium and PTFE) were used in the construction of the capsule and post-dispersion duct, as shown in

Figure 2. The particles impact not only on the capsule walls, but also on the post-dispersion duct after leaving the dispersion capsule. Therefore the same material of construction was used for both components. The experiments were carried out on 53-63 µm glass ballotini at the dispersion pressure of 2 barg and using 3 mm^3 of sample volume. The results are shown in Figure 7.

The polarity of the charge on the particles is negative for copper, steel, brass and aluminium, and positive for PTFE. The largest level of charge is observed with PTFE, while the highest negative charge is given by the copper capsule. The difference in charging of glass ballotini against different metal surfaces is due to their work function which is generally determined by Photo-Emission Spectroscopy (PES) and Kevin-Zisman method. Metals having a higher work function, i.e. copper (~5.1 eV) and stainless steel (~4.67 eV) transfer a greater negative charge compared to brass (~4.5 eV) and aluminium (~4.06 eV) (Carter et al., 1992) and (Matsusaka et al., 2010). The PTFE surface has a higher work function than that of the glass ballotini and therefore it is expected that electrons are transferred from the glass ballotini to the PTFE surfaces, resulting in the particles acquiring a positive charge (Elajnaf et al., 2006), and (He et al., 2014).

These results are in good agreement with the work of Šupuk et al. (2012) and Zarrebini et al. (2013) who investigated the effect of same materials on triboelectric charging of glass ballotini using different charge transfer methods.

Effect of surface functional groups

Triboelectric charging is a surface phenomenon and is strongly influenced by the functional groups exposed on the surface. Glass ballotini (sieve cut: 53-63µm), coated with different functional groups, have been tested to verify the effect of surface functionalisation on tribo-electrification. The silanisation process is used for this purpose, where the particles surfaces are covered by self-assembling of alkoxysilane molecules (Seed, 2001). Three different functional groups have been used: -CF3, -CH3, -NH2. The charge-to-mass ratio has been measured against stainless steel surface with an air pressure pulse of 2 barg to ensure an efficient dispersion. A sample volume of 3 mm^3 was used for each test. The results are presented in Figure 8 and show that surface functionalisation has indeed a great influence on contact charging.

The glass ballotini covered with –CF3 charge negatively and the magnitude of charge is very high indeed (−1584 nC/g), while the other two surface groups charge positively. The particles coated with –NH2 get a higher amount of charge (537 nC/g) compared to the ones coated with –CH3 (185 nC/g). The trends are consistent with the work of Wang et al. (2016) on the same functional groups. This can be explained by the electro-negativity of –CF3 group (it has the highest electronegativity according to Huheey, 1965 and Deryagin et al. (1978), as it is a strong electron acceptor, while –NH2 is an electron donor (Morra et al., 1990) and (Trigwell et al., 2003). Wang et al. (2016) used this method to enhance the power output of triboelectric nano-generators.

Tribo-electrification of Pharmaceutical Powders

Pharmaceutical industry is particularly vulnerable to particle handling problems created by electrostatic charge as organic crystals are commonly dielectric and retain charges brought about by tribo-electrification, causing segregation and flowability issues during processing. Therefore, the ability to test a small quantity of the drug for charging at the early stages of drug development is highly desirable. The performance of the method for a number of organic crystals has been tested and is reported below.

Aspirin and α-Lactose monohydrate

The relationship between the absolute value of the acquired charge, |Q|, and the quantity of the particles, represented by the estimated number of particles, Np, was investigated using aspirin and α-lactose monohydrate. The dispersion pressure was set at 2 barg and bulk sample volumes 1, 3, 5, 7 mm^3 were used. Both materials charged negatively against stainless steel. For each volume, the number of particles in the sampling spoon was roughly estimated by dividing their total volume by the estimated volume of a single particle. The total volume of the solids in the spoon was calculated by dividing the measured mass of the powder by the true density of the material (1400 kg.m^{-3} for aspirin and 1525 kg.m^{-3} for α-lactose monohydrate) while the volume of a single particle was calculated assuming that the particles were spheres with a diameter equal to the volume mean diameter (D[4,3]) measured by laser diffraction analysis (LDA), as shown in Table 2, where other measures of the particle distribution are also given. The final charge acquired by the sample after the dispersion process as a function of the estimated number of particles is shown in Figure 9 for aspirin and for α-lactose monohydrate. The number of particles is of course only an estimate; nevertheless a remarkably linear relationship is

observed in both cases. The acquired charge for single particles by extrapolation of the lines is estimated as −44 pC for aspirin and −19 pC for α-lactose monohydrate These values are remarkably in close agreement with those reported by Watanabe et al. (2006), using the Single Particle Impact Tester. In their work the value of the charge acquired by a single particle after impact on a stainless steel plate (impact charge) was reported as a function of the initial particle charge. Various pharmaceutical powders were tested and the "equilibrium charge", i.e. the value of the initial charge for which no further charge transfer takes place, was reported. The equilibrium charge is independent of the impact velocity and can be considered as the maximum charge that a particle can get. They reported the equilibrium charge as $Q_e = -40.1$ pC for aspirin and $Q_e = -18.1$ pC for α-lactose monohydrate. These values are close to those measured with the dispersion device here, thus suggesting that the particles approach the equilibrium charge level.

Effect of Crystallisation Process on Triboelectric Charging

During the crystallisation process, a number of factors influence the physical and chemical properties of the final product, such as solvent, cooling rate, amount of seeding, etc (Nguyen et al., 2017), (Kashchiev et al., 2010) and (Stoica et al., 2004). The solvent, for example, affects the super-saturation, the nucleation rate and growth rate of each crystal face, which in turn influence the size and morphology of the crystals, their purity and aggregation/agglomeration behaviour (McLachlan and Ni, 2016), (Beck et al., 2009) and (Granberg et al., 1999). In this work, Paracetamol, Metacetamol, urea, L-glutamic acid and carbamazepine have been tested to investigate the effect of crystallisation process on triboelectric charging properties.

Paracetamol and Metacetamol

Paracetamol, Metacetamol (a structural isomer of Paracetamol), and mixtures of 98% Paracetamol and 2% Metacetamol by weight, crystallised together by various solvents, were used to quantify the polarity and magnitude of triboelectric charging during dispersion. Scanning Electron Microscope (SEM) images of the crystals are shown in Figure 10. The designation numbers in Table 3 relate to the crystal systems shown in Figure 10. Pure Metacetamol has an acicular shape, unlike Paracetamol. The use of isopropyl alcohol (IPA) as solvent causes a notable reduction in particle size due to higher supersaturation during crystallisation compared to the other solvents (see case 4 in Figure 10). For charge measurement, the samples were dispersed at 2 barg dispersion pressure and 20 ms pulse time period using a volume of 5 mm^3. All the measurements produced negative charge on the crystals and the results are shown in Figure 11. The effect of different mixtures and solvents on charging clearly seen. Paracetamol crystallised with only water (case 1) exhibits the lowest charge-to-mass ratio compared to when crystallised from a solvent mixture of 50% water - 50 % ethanol (case 2). Furthermore, the highest charge-to-mass ratio is obtained for a mixture 98% Paracetamol and 2% Metacetammol crystallised with IPA solvent (case 4), which produces the finest particle size distribution (average D[3,2] of 33 µm, see Table 3) As it can be seen in Figure 10, particle size is strongly affected by the solvent type, and this in turn effects the charging tendency significantly. However, the specific charge per unit mass as presented above does not account for particle size change. As triboelectric charging is a surface phenomenon, an attempt was made to account for the change in particle size by characterising the specific surface area of the test powders. This was measured by BET surface area analyser (Quantachrome Instruments, Florida, USA) and also separately inferred from the particle size analysis based on laser diffraction. The comparison between the average values obtained for

charge per unit mass (nC/g) and charge per unit surface area ($\mu C/m^2$) for the Paracetamol-Metacetamol system is shown in Table 3. As intuitively expected, the trend of charging tendency in the case of charge per unit surface area is different compared to charge per unit mass. According to the result, the Paracetamol sample crystallised with the mixture of water and ethanol yields the highest charge per unit surface area compared to other solvent mixtures and pure solvents. The second highest is for 98% Paracetamol with 2% Metacetamol sample crystallised with 50-50 water - IPA. Clearly solvent type and composition have a significant influence on charging. It is noteworthy that the estimation of the specific surface area based on particle size analysis by LDA led to similar values to those from BET analysis (not shown here for brevity) and therefore the charge per unit surface area from both techniques were similar. Further in depth investigation is required to understand the effect of solvents and impurities on tribo-electric charging of organic materials. However, the proposed technique can readily characterise the triboelectric charge of the particles having changes in the crystallisation process.

Urea

The effect of solvent used for the crystallisation process of urea on its charging propensity has been investigated by testing five samples of urea crystals made from different solvents: ethanol, methanol and isopropyl alcohol. The SEM images of the crystals are shown in Figure 12. The designation number for each image is also used for Table 4. The effect of adding biuret (a chemical compound usually considered as an impurity in urea-based fertilizers) during crystallisation with ethanol has also been evaluated. The results are shown in Figure 13.

All the samples charge negatively; the highest charge to mass ratio is acquired by the sample crystallised in IPA, similar to the case of Paracetamol, while the lowest is by the sample crystallised in methanol. The addition of biuret in the crystallisation process with ethanol seems to reduce drastically the charge pick up and also change the morphology of the crystals. As with the case of Paracetamol, the specific surface area of urea was analysed by BET and also inferred from LDA. The particle size, specific surface area and charging characteristics of urea crystallised from three solvents: ethanol (with and without addition of biuret), methanol and IPA are shown in Table 4. The charge per unit surface area ($\mu C/m^2$) has a very different trend compared to the charge per unit mass, (nC/g). Urea crystals from ethanol (case 1) yield the highest charging tendency in terms of charge per unit surface area, whilst the least charging is recorded for urea with 8% biuret from ethanol (case 3). It was found that the specific surface area obtained by the two methods had a large difference. The BET analysis is considered more reliable as the particle size analysis by LDA for high aspect ratio crystals is associated with large errors. Therefore it is not shown here. A more in-depth analysis of the surface functional group would be needed to interpret the trend observed here.

L-Glutamic Acid

The effect of crystallisation process conditions on triboelectric charging was further evaluated for L-glutamic acid. This crystal system has two different forms, α and β, which differ in the structure of the molecule. The two forms can be obtained by crystallisation in water using high or low cooling rates, respectively. The shapes of these two forms are very different with the β form more elongated and needle-like. The charge-to-mass ratio of the two samples of L-glutamic acid is shown in Figure 14. Both forms charge negatively and the β form acquires a higher amount of charge. A similar trend has previously been reported by Karner et al. (2014)

for other active pharmaceutical ingredients (APIs) with high aspect ratios. However, the underlying mechanisms giving rise to the difference in the magnitude of charge require a study of the functional groups on the crystal surface. Nevertheless, the proposed tribo-electric charge measurement device can successfully diagnose these differences.

Carbamazepine

Carbamazepine has four anhydrous polymorphs and one dihydrate form, which differ in several physical and chemical properties, such as solubility, stability and hygroscopicity. Two different forms have been tested here in order to assess the difference in contact charging behaviour: dihydrate and anhydrous (P-monoclinic, form III). The results are reported in Figure 15 and show that the two forms charge with opposite polarities: the dihydrate form charges positively and the anhydrous one charges negatively with a higher magnitude, presumably due to difference in surface functional groups.

4. Conclusions

The potential of using a pulse of pressurised gas to disperse a small powder quantity to assess the triboelectric charging propensity is explored. The technique is highly sensitive; only a small quantity of sample is required (as small as a few microgram), with no charge losses as the powder is directly dispersed into a Faraday cup, and providing rapid testing. The proposed technique can be successfully used to quantify charging propensity of powders having changes, such as different polymorphs, morphology, crystallisation routes and functional surface groups.

5. Acknowledgements

6. References

Ali, M., Ghadiri, M., 2017. Analysis of triboelectric charging of particles due to aerodynamic dispersion by a pulse of pressurised air jet. Advanced Powder Technology, 28 (10), 2735-2740.

Ali, M., Reddy, R.N., Mazumder, M.K., 2008. Electrostatic charge effect on respirable aerosol particle deposition in a cadaver based throat cast replica. Journal of Electrostatics. 66 (7), 401–406.

Beck, R., Hakkinen, A., Sorenssen, M.D., Andreassen, P.J., 2009. The effect of crsytallization condition, crystal morphology and size on pressure filtration of L-glutamic acid and an aromatic amine. Separation and Purification Technology, 66, (3), 549-558.

Biegaj, K., Kwek, J.W., Lukar, T., Rowland, M., Heng, J.Y.Y., 2016. Novel Coupling of a Capacitive Probe with a Dynamic Vapor Sorption (DVS) Instrument for the Electrostatic Measurements of Powders, Industrial & Engineering Chemistry Research, 55,5585-5589.

Brown, R.C., 1997. Tutorial review: simultaneous measurement of particle size and particle charge. Journal of Aerosol Science. 28 (8), 1373–1391.

Coudray, N., Dieterlen, A., Roth, E., Trouvé, G., 2009. Density measurement of fine aerosol fractions from wood combustion sources using ELPI distributions and image processing techniques. Fuel, 88, 947–954.

Carter, P., Rowley, G., Fletcher, E., Hill, E., 1992. An experimental investigation of triboelectrification in cohesive and non-cohesive pharmaceutical powders. Drug Development Industrial Pharmacy. 18 (14), 1505–1526.

Chilworth Instruments., 2018. [online], available at: http://www.dekra-process-safety.co.uk/instruments/jci-electrostatic-instruments/jci147-faraday-pail [Accessed 5th Jan. 2018].

Chow, K.T., Zhu, K., Tan, R.B.H., Heng, P.W.S., 2008. Investigation of electrostatic behavior of a lactose carrier for dry powder inhalers. Pharmaceutical Research. 25 (12), 2822– 2834.

Deryagin, B.V., Krotova, N.A., Smilga'V, P., 1978. Adhesion of Solids. Consultants Bureau, New York, NY.

Elajnaf, A., Carter, P., Rowley, G., 2006. Electrostatic characterisation of inhaled powders: effect of contact surface and relative humidity. European Journal of Pharmaceutical Sciences. 29 (5), 375–384.

Elsdon, R., and Mitchell, F., 1976, Contact Electrification of Polymers, Journal of Physics D: Applied Physics, 9, 1445-1460.

Ema, A., Yasuda, D., Tanoue, K., and Masuda, H., 2003. Tribo-Charge and Rebound Characteristics of Particles Impact on Inclined or Rotating Metal Target, Powder Technology, 2-13

Epping, R.H., Kuettner, A., 2002. Free air beam in an electric field for determination of the electrostatic charge of powders between 1 and 200 µm. Journal of Electrostatics. 55, 279-288.

Granberg, Roger A., Dan G. Bloch, and C. Rasmuson. 1999. "Crystallisation of Paracetamol in Acetone — Water Mixtures." 198/199:1287–93

Gupta, R., Gidaspow, D., and Wasan, D.T., 1992. Electrostatic Separation of Powder Mixtures Based on the Work Function of its Constituents, Powder Technology, 75, 79-87

Harper, W.R., 1967. Contact and Frictional Electrification. Clarendon P, Oxford.

He, C., Bi, X.T., Grace, J.R., 2014. Contact electrification of a novel dual-material probe with charged particulate flow, Powder Technology, 253, 1-9.

Hoe, S., Traini, D., Chan, H., Young, P.M., 2009. Influence of flow rate on the aerosol deposition profile and electrostatic charge of single and combination metered dose inhalers. Pharmaceutical Research. 26 (12), 2639–2646.

Huheey, E.J., 1965. The Electronegativity of Groups. The Journal of Physical Chemistry 69(10), 3284–3291.

Hussain T., Deng T., Bradley M.S.A., Armour-Chélu D., Gorman T., Kaialy W., 2016. Evaluation studies of a sensing technique for electrostatic charge polarity of pharmaceutical particulates, IET Science, Measurement & Technology, 10 (5), 442-448,

Itakura, T., Masuda, H., Ohtsuka, C., and Matsusaka, S., 1996. The Contact Potential Difference and the Tribo-Charge, Journal of Electrostatics. 38, 213-226.

Karner, S., Littringer, E.M., Urbanetz, N.A., 2014. Triboelectrics: the influence of particle surface roughness and shape on charge acquisition during aerosolization and the DPI performance. Powder Technology. 262, 22–29.

Kashchiev, D., Borissova, A., Hammond, R.B., Roberts, K. J., 2010. Effect of cooling rate on the critical undercooling for crystallisation. Journal of Crystal Growth, 312:698-704.

Kwek, J.W., Ng, W.K., Tan, R.B.H., Jeyabalasingam, J.Y.Y., Heng, R.B.H., 2012. Comparative study of the triboelectric charging behavior of powders using a nonintrusive approach. Industrial and Engineering Chemistry Research. 51 (50), 16488–16494.

Kwok, P., Glover, W., Chan, H., 2005. Electrostatic charge characteristics of aerosols produced from metered dose inhalers. Journal of Pharmaceutical Science. 94 (12), 2789–2799.

Kwek, J.W., Ng, W.K., Tan, R.B.H., Jeyabalasingam, J.Y.Y., Heng, R.B.H., 2012. Comparative study of the triboelectric charging behavior of powders using a nonintrusive approach. Industrial and Engineering Chemistry Research. 51 (50), 16488–16494.

Leung, S., Chiow, A., Ukkonen, A., Chan, H., 2016. Applicability of bipolar charge analyzer (BOLAR) in characterizing the bipolar electrostatic charge profile of commercial metered dose inhalers (MDIs). Pharmaceutical Research. 33 (2), 283–291.

Masuda, H., Iinoya, K., 1978. Electrification of particles by impact on inclined metal plates. AIChE J. 24 (6), 950–956.

Masuda, H., Itakura, T., Gotoh, K., Takahashi, T., Teshima, T., 1995. The measurement and evaluation of the contact potential difference between various powders and a metal. Advance Powder Technology. 6, 295-303.

Masui, N., Murata, Y., 1983. Electrification of polymer particles by impact on a metal plate. Japan Journal Applied Physics. 22, 1057–1062.

Matsusaka, S., Ghadiri, M, Masuda, H., 2000. Electrification of an elastic sphere by repeated impacts on a metal plate. Journal of Physics D: Applied Physics 33, 2311-2319.

Matsusaka, S., Maruyama, H., Matsuyama, T., Ghadiri, M., 2010. Triboelectric charging of powders: a review. Chemical and Engineering Science. 65 (22), 5781–5807.

Matsusaka, S., and Masuda, H. (2003), Electrostatics of Particles, Advance Powder Technology. 14, 143-166.

Matsuyama, T., Yamamoto, H., 1995. Characterizing the electrostatic charging of polymer particles by impact charging experiments. Advance Powder Technology. 6 (3), 211–220.

McLachlan, H., Ni, X., 2016. On the effect of added impurity on crystal purity of urea in an oscillatory baffled crystallizer and a stirred tank crystallizer. Journal of Crystal Growth, 442, 81-88.

Morra, M., Occhiello, E., Garbassi, F., 1990. Surface characterization of plasma-treated PTFE. Surface and Interface Analysis. 16 (1–12), 412–417.

Mukherjee, R., Gupta, V., Naik, S., Sarkar, S., Sharma, V., Peri, P. and Chaudhuri, B., 2016. Effects of particle size on the triboelectrification phenomenon in pharmaceutical excipients: Experiments and multi-scale modelling. Asian Journal of Pharmaceutical Sciences. 11 (5), 603-617.

Murtomaa, M., Strengell, S., Laine, E., Bailey, A., 2003. Measurement of electrostatic charge of an aerosol using a grid- probe. Journal of Electrostatics. 58 (3), 197–207.

Naik, S., Mukherjee, R., Chaudhuri, B., 2016. Triboelectrification: A review of experimental and mechanistic modelling approaches with a special focus on pharmaceutical powders. International Journal of Pharmaceutics. 510, 375-385.

Nguyen, T. T. H., Rosbottom, I., Marziano, I., Hammond, R. B., Roberts, K. J., 2017. Crystal Morphology and Interfacial Stability of RS-Ibuprofen in Relation to Its Molecular and Synthonic Structure. Crystal Growth & Design. 17, (6), 3088-3099.

Pingali, K.C., Shinbrot, T., Hammond, S.V., Muzzio, F.J., 2009. An observed correlation between flow and electrical properties of pharmaceutical blends. Powder Technology. 192 (2), 157–165.

Rowley, G., 2001. Quantifying electrostatic interactions in pharmaceutical solid systems. International Journal of Pharmaceutics. 227 (1), 47–55.

Saini, D., Trigwell, S., Srirama, P.K., Sim, A.R., Sharma, R., Biris, S.A., 2008. Portable free-fall electrostatic separator for beneficiation of charged particulate materials. Particulate Science and Technology. 26 (4), 349–360.

Sarkar, S., Cho, J., Chaudhuri, B., 2012. Mechanisms of electrostatic charge reduction of granular media with additives on different surfaces. Chemical Engineering and Processing: Process Intensification. 62, 168

Seed, B., 2001. Silanizing Glassware. Current Protocols in Cell Biology 8 (3) E:A.3E. 1-A.3E 2.

Smyth HD., Cooney, D., Garmise, RJ., Zimmerer, RD., Pipkin, JD., and Hickey, AJ., 2004. Dynamic electrostatic charge derminations of dry powder blends for inhalation: Correlation with dispersion performance. Respiratory Drug Delivery IX. 3, 805-808.

Stoica, C., Verwer, P., Meekes, H., Van Hoof, P.J.C.M., Kaspersen, F.M., Vleig, E., 2004. Understanding the effect of a solvent on the crystal habit. Crystal Growth & Design, 4, (4), 765-768.

Šupuk, E., Zarrebini, A., Reddy, J.P., Hughes, H., Leane, M.M., Tobyn, M.J., Timmins, P., Ghadiri, M., 2012. Tribo-electrification of active pharmaceutical ingredients and excipients. Powder Technology. 217, 427–434.

Telko, M.J., Kujanpää, J., Hickey, A.J., 2007. Investigation of triboelectric charging in dry powder inhalers using electrical low pressure impactor (ELPI). International Journal of Pharmaceutics. 336 (2), 352–360.

Trigwell, S., Grable, N., Yurteri, C.U., Sharma, R., Mazumder, M.K., 2003. Effects of surface properties on the tribocharging characteristics of polymer powder as applied to industrial processes. IEEE Transactions and Industry Applications. 39 (1), 79–86.

Wang, S., Zi, Y., Zhou, S.Y., Li, S., Fan, F., Lin, L., Wang, L.Z., 2016. "Molecular Surface Functionalization to Enhance the Power Output of Triboelectric Nano generators." Journal of Materials Chemistry. A, 4, 3728-3734.

Watanabe, H., Ghadiri, M., Matsuyama, T., Ding, Y.L., Pitt, K.G., Maruyama, H., Matsusaka, S., Masuda, H., 2007. Triboelectrification of pharmaceutical powders by particle impact. International Journal of Pharmaceutics. 334 (1), 149–155.

Watano, S., 2006. Mechanism and control of electrification in pneumatic conveying of powders. Chemical Engineering Science. 61, 2271-2278.

Wong, J., Kwok, P.C.L., Noakes, T., Fathi, A., Dehghani, F., Chan, H., 2014. Effect of crystallinity on electrostatic charging in dry powder inhaler formulations. Pharmaceutical Research. 31 (7), 1656.

Wong, J., Lin, Y., Kwok, P.C.L., Niemel, V., Crapper, J., Chan, H., 2015. Measuring bipolar charge and mass distributions of powder aerosols by a novel tool (BOLAR). Molecular Pharmaceutics. 12 (9), 3433.

Yli-Ojanperä, J., Ukkonen, A., Järvinen, A., Layzell, S., Niemelä, V., Keskinen, J., 2014. Bipolar charge analyzer (BOLAR): A new aerosol instrument for bipolar charge measurements. Journal of Aerosol Science. 77, 16–30.

Yurteri, C.U., Mazumder, M.K., Grable, N., Ahuja, G., Trigwell, S., Biris, A.S., Sharma, R., and Sims, R.A. (2002), Electrostatic Effects in Dispersion, Transport, and Deposition of Fine Pharmaceutical Powders: Development of an Experimental Method for Quantitative Analysis, Particulate Science and Technology. 20, 59-79

Zarrebini, A., Ghadiri, M., Dyson, M., Kippax, P., and McNeil-Watson, F., 2013. Triboelectrification of powders due to dispersion. Powder technology 250: 75-83.

Zhao, H., Castle, G.S.P., Inculet, I.I., 2002. The measurement of bipolar charge in polydisperse powders using a vertical array of faraday pail sensors. Journal of Electrostatics. 55 (3), 261–278.

Zhou Y.S., Liu Y., Zhu G., Lin Z.H., Pan C., Jing Q., Wang Z.L., 2013. In Situ Quantitative Study of Nanoscale Triboelectrification and Patterning, Nano Letters, Volume 16, p.2771-2776.
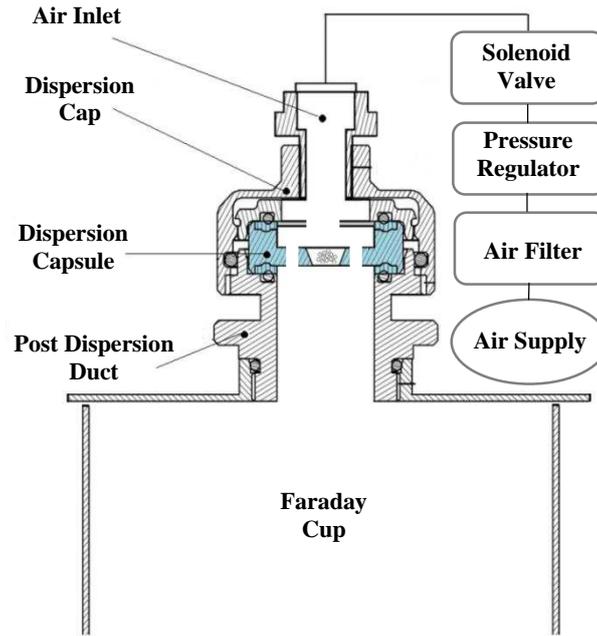
Figure 1: Schematic diagram of the dispersion setup for assessing tribo-electric charging of particles.

Figure 2: Post-dispersion ducts (top) and dispersion capsule (bottom) made of five different materials: copper, stainless steel, brass, aluminium and PTFE.
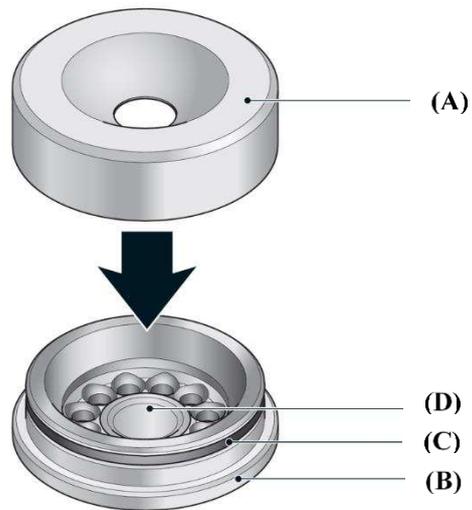
Figure 3: (A) Top section of the dispersion capsule; (B) Bottom section of the capsule; (c) O-ring; (D) Sample well (Malvern® Instruments Ltd, 2013)
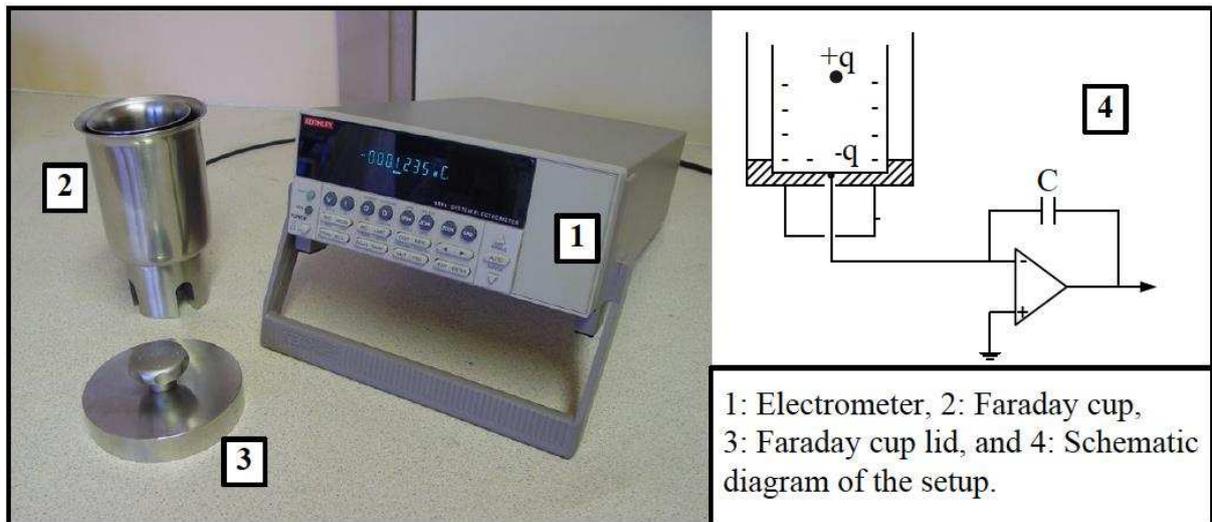

1: Electrometer, 2: Faraday cup, 3: Faraday cup lid, and 4: Schematic diagram of the setup.

Figure 4: Charge measurement set-up used in the study.
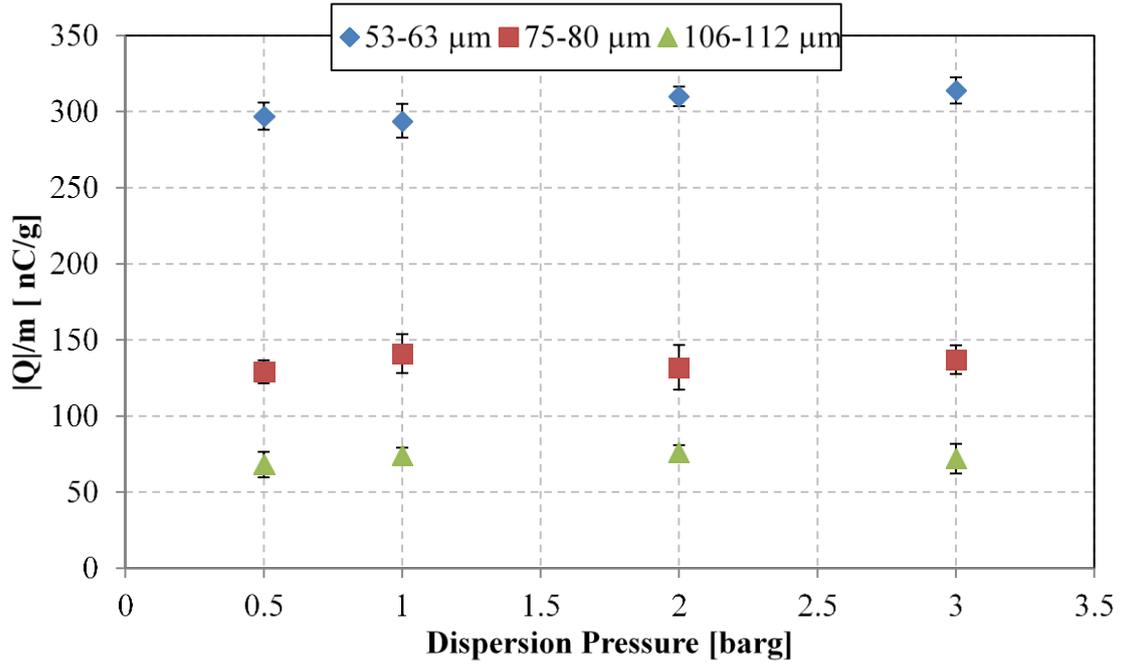
Figure 5: Absolute magnitude of charge-to-mass ratio of glass ballotini against stainless steel surface as a function dispersion pressure for three different sieve cuts, using 3 mm^3 sample volume.
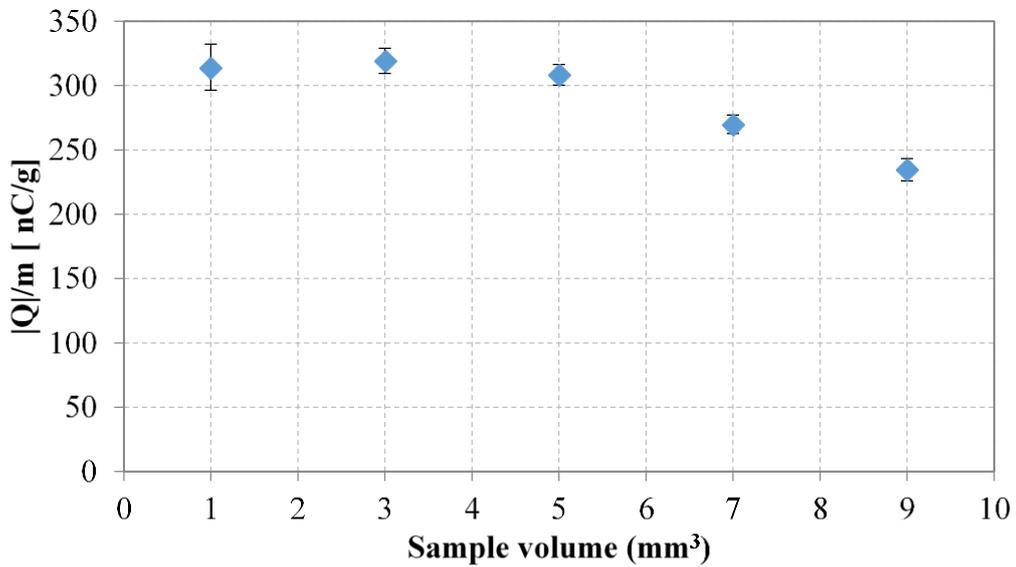
Figure 6: Absolute magnitude of the charge to mass ratio as a function of sample volume for glass ballotini of sieve cut 53-63 µm against stainless steel surface at 2 barg dispersion pressure.
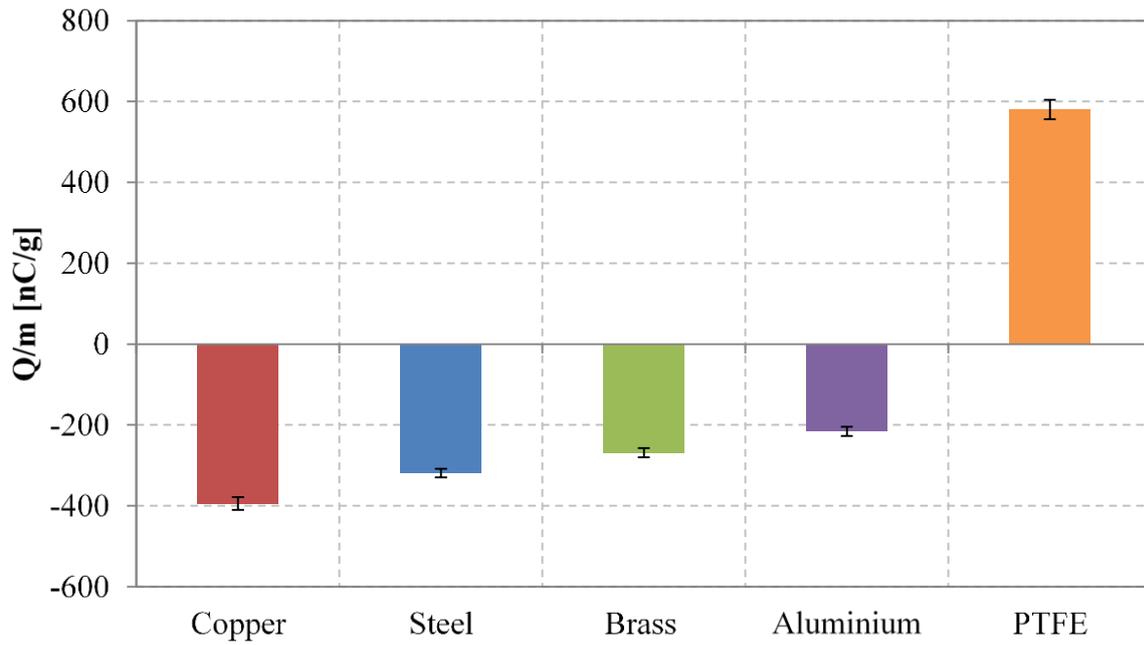
Figure 7: Charge-to-mass ratio for 53-63 µm glass ballotini contacting different surface materials during dispersion at 2 barg pressure and 3 mm^3 sample volume.
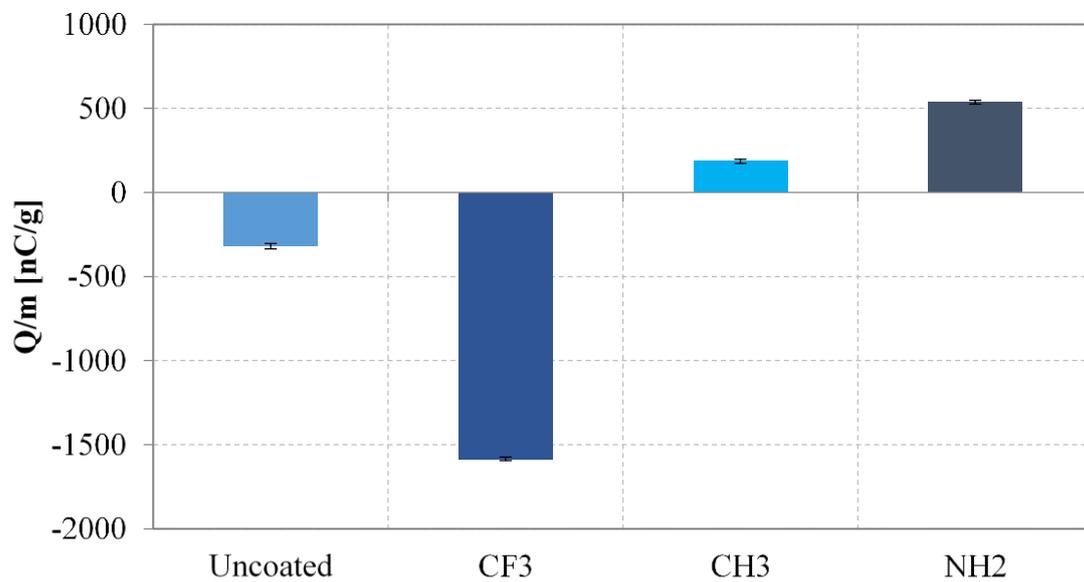
Figure 8: Charge-to-mass ratio of glass ballotini covered with functional groups (-CF3, -CH3, -NH2) against stainless steel surface at 2 barg and 3 mm^3.
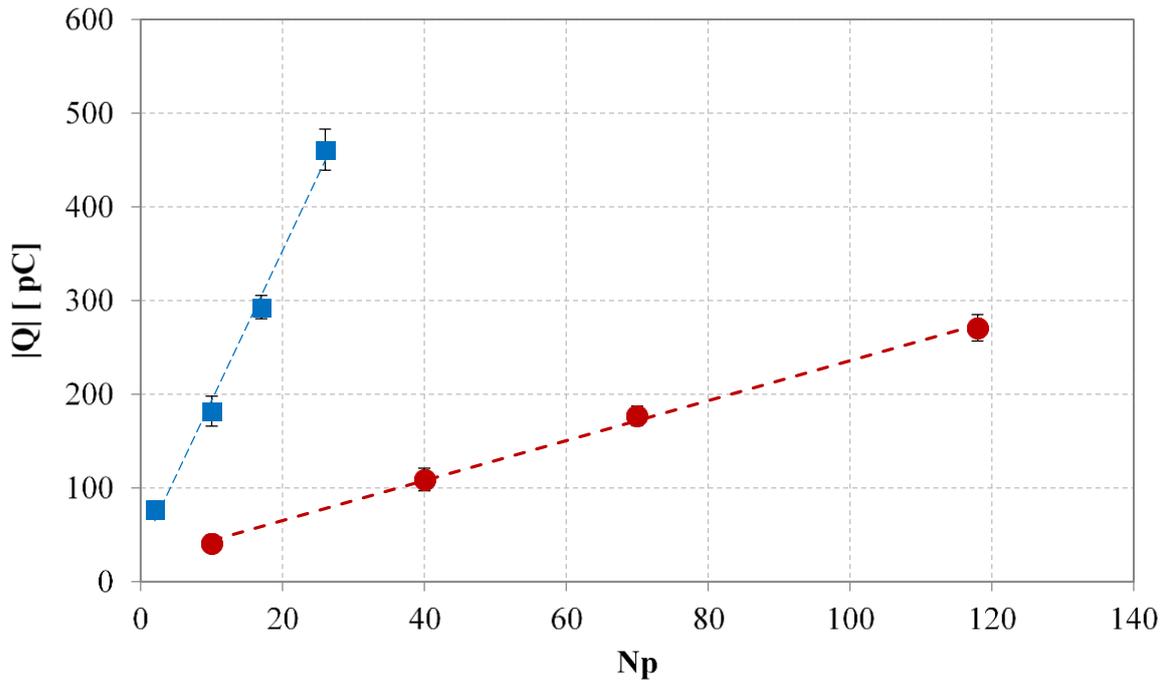
Figure 9: Relationship between the estimated number of particles $N_p \geq 1$ and the absolute value of the sample charge. ■: aspirin and ●:α-lactose monohydrate.
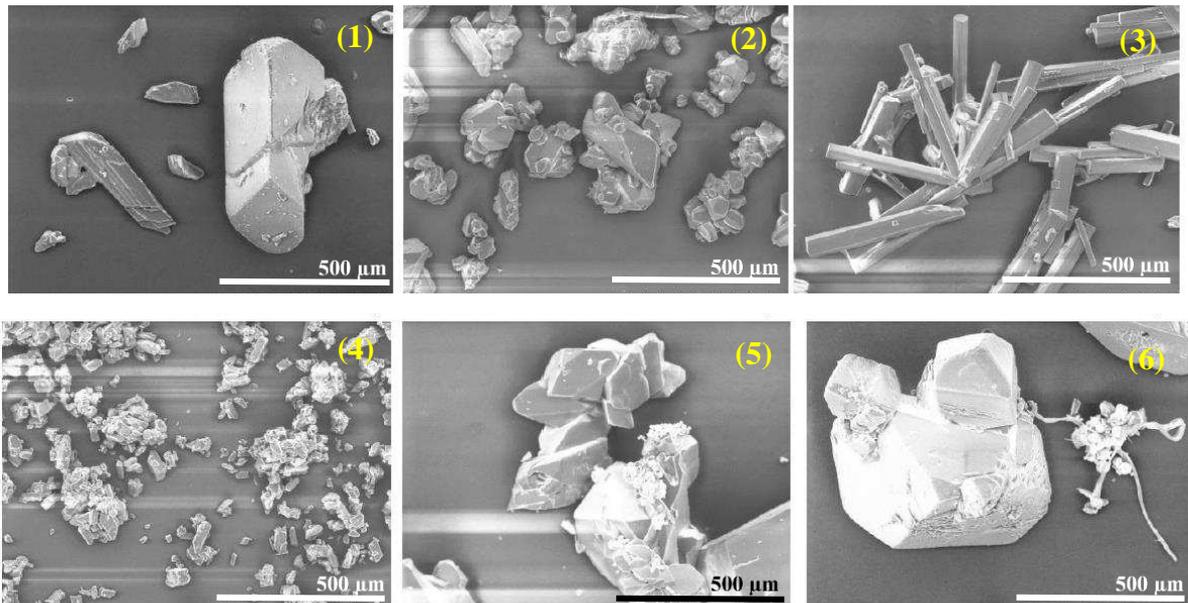

Figure 10: SEM images of Paracetamol, Metacetamol and their mixtures at 150 × magnification (from left to right): (1) : 100% Paracetamol in 100% Water, (2) : 100% Paracetamol in 50% Water 50% Ethanol, (3) : 100% Metacetamol in 100% IPA, (4) : 98% Paracetamol 2% Metacetamol in 100% IPA, (5) : 98% Paracetamol 2% Metacetamol in 50% Water 50% IPA, (6) : 98% Paracetamol 2% Metacetamol in 100% Water.
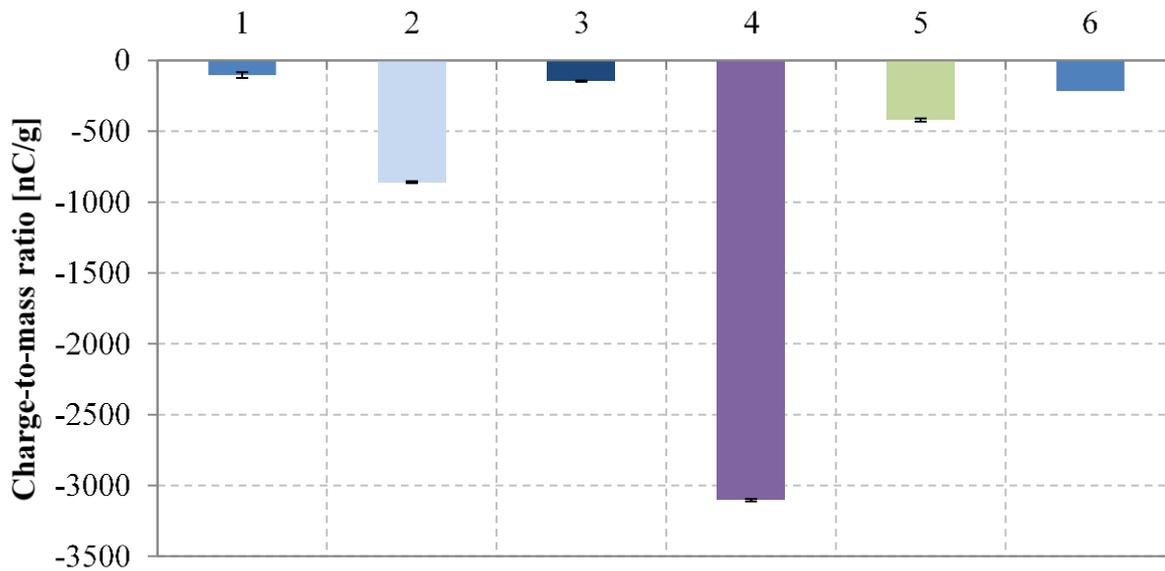
Figure 11: Charge per unit mass for crystals of Paracetamol, Metacetamol and their mixtures produced from different solvents: (1) : 100% Paracetamol in 100% Water, (2) : 100% Paracetamol in 50% Water 50% Ethanol, (3) - 100% Metacetamol in 100% IPA, (4) : 98% Paracetamol 2% Metacetamol in 100% IPA, (5) : 98% Paracetamol 2% Metacetamol in 50% Water 50% IPA, (6): 98% Paracetamol 2% Metacetamol in 100% Water.
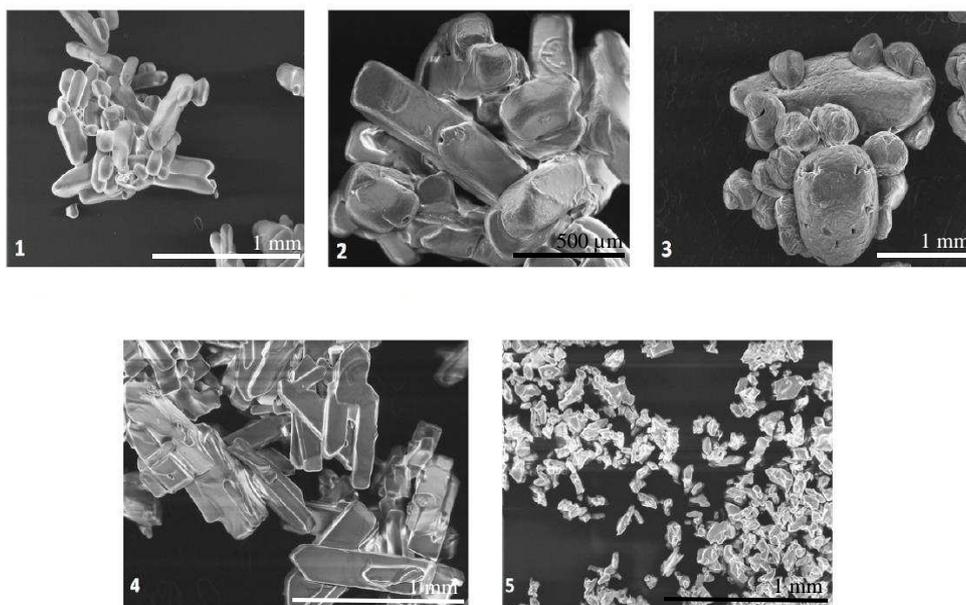
Figure 12: SEM images of five samples of urea crystallised from different solvents: (1): ethanol, (2): ethanol with 4% of biuret, (3): ethanol with 8% of biuret, (4): methanol and (5) isopropyl alcohol.
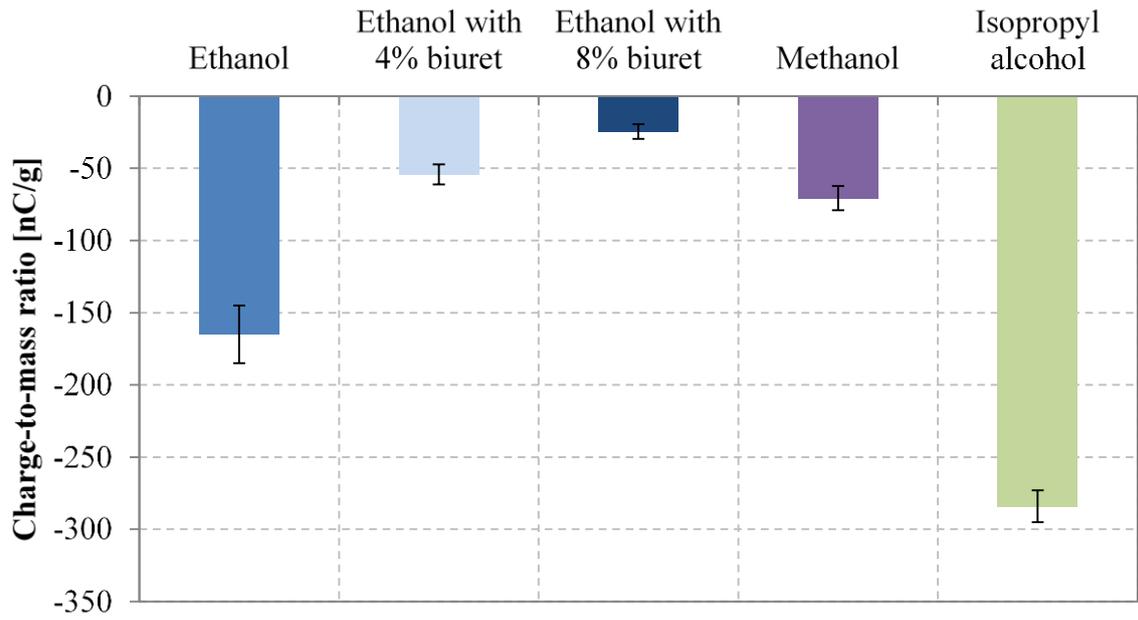
Figure 13: Charge-to-mass ratio of urea crystals, produced from different solvents and with biuret as impurity, measured at 2 barg using 3 mm^3 sample volume.
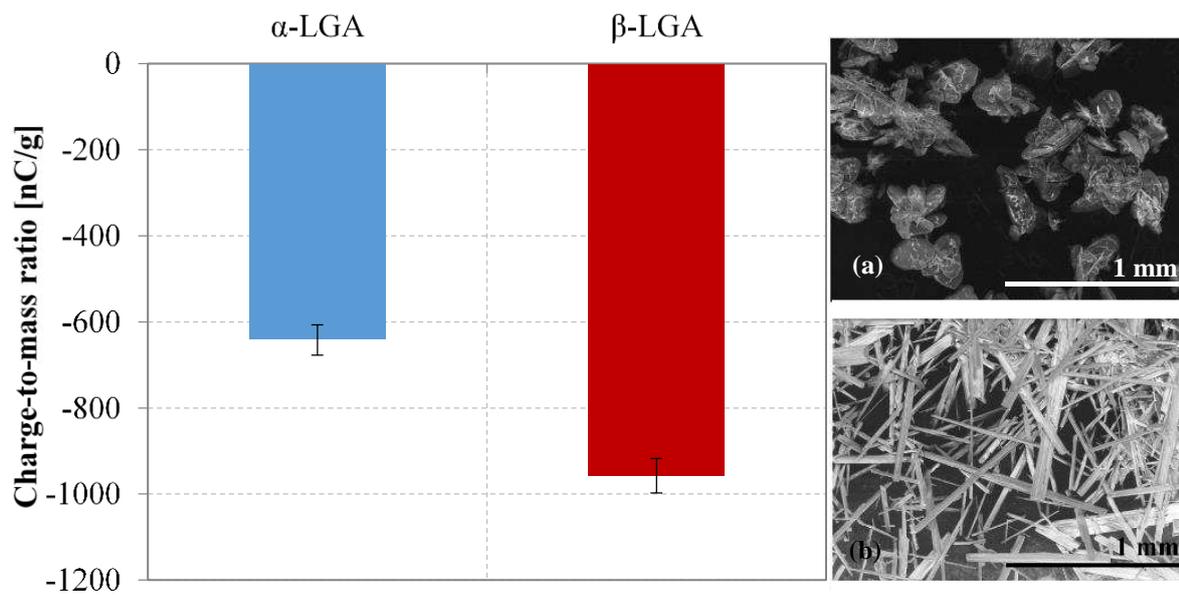
Figure 14: Charge to mass ratio of two different forms of L-glutamic acid along with their SEM images (a) α-form (b) β-form.
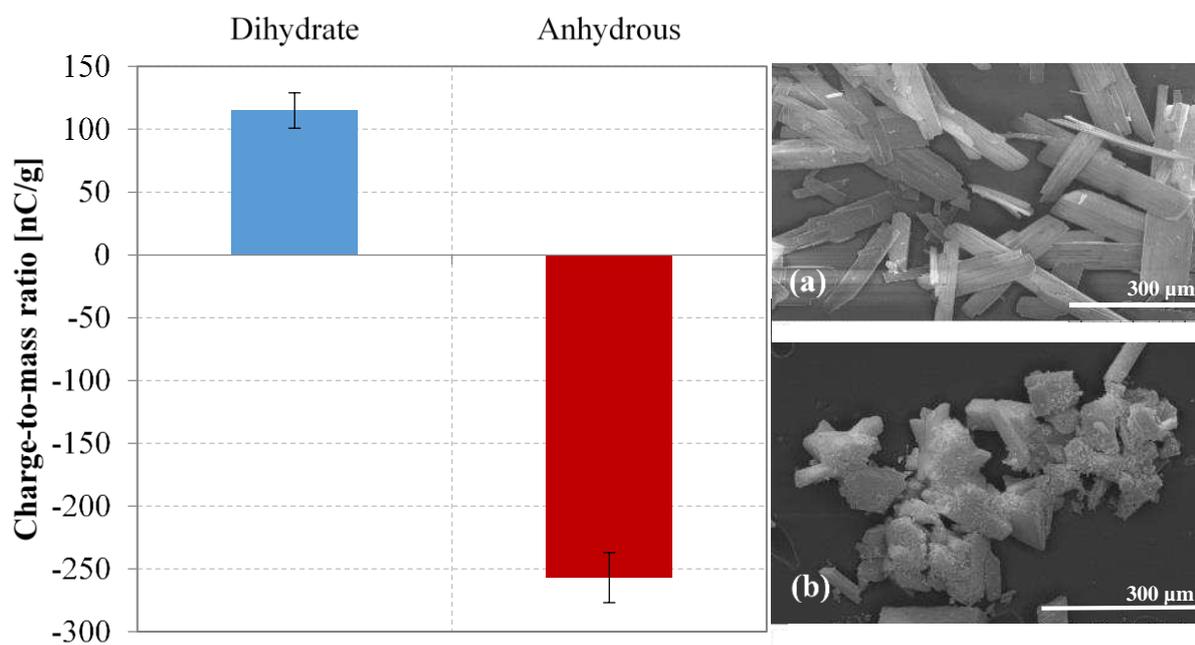
Figure 15: Charge-to-mass ratio of two different forms of carbamazepine along with SEM images (a) dehydrate (b) anhydrous (P-monoclinic, form III).

Table 1: Characteristic measures of particle size distributions of glass ballotini obtained by laser diffraction using the wet dispersion method (volume basis) and charging characteristics.

Glass ballotini / Size (µm)	D[3,2]	$D_{v,10}$	$D_{v,50}$	$D_{v,90}$	Specific surface area, m^2/g	Charge per unit mass, nC/m^2	Charge per unit surface area, $\mu C/m^2$
53-63	50	47	56	70	0.048	303.7	6328
75-80	78	65	82	98	0.031	134.7	4379
106-112	107	97	111	129	0.022	72.5	3232

Table 2: Characteristic measures of particle size distributions obtained by laser diffraction analysis using wet dispersion (volume basis) for aspirin and α-lactose monohydrate.

Material / Size (µm)	D[4,3]	D[3,2]	$D_{v,10}$	$D_{v,50}$	$D_{v,90}$
Aspirin	693	622	424	663	1006
α-lactose monohydrate	397	335	262	381	554

Table 3: Particle size, specific surface area and charging characteristics of
Paracetamol/Metacetamol systems.

Material Designation, c.f. Figure 10	D[3,2], μm	Specific surface area m²/g	Charge per unit mass (nC/g)	Charge per unit surface area (μC/m²)
1	659	0.007	-103	-13.6
2	198	0024	-860	-35.4
3	96	0.021	-146	-6.8
4	33	0.143	-3103	-21.7
5	385	0.014	-421	-29.9
6	408	0.023	-216	-9.3

Table 4: Particle size, specific surface area and charging characteristics of urea crystallised in
ethanol (with addition of biuret as impurity), methanol and IPA.

Material Designation, c.f, Figure 12	D[3,2], μm	Specific surface area m²/g	Charge per unit mass (nC/g)	Charge per unit surface area (μC/m²)
1	223	0.03	-165	-5.9
2	430	0.06	-54.3	-0.9
3	578	0.88	-24.6	-0.03
4	157	1.23	-70.6	-0.06
5	27	1.80	-284	-0.16